Title
HONO decomposition on borosilicate glass surfaces: implications for environmental chamber studies and field experiments

Journal
Physical Chemistry Chemical Physics, 5(23)

ISSN
1463-9076 1463-9084

Authors
Syomin, Dennis A
Finlayson-Pitts, Barbara J

Publication Date
2003

DOI
10.1039/b309851f

Peer reviewed

PCCP

HONO decomposition on borosilicate glass surfaces: implications for environmental chamber studies and field experiments

Dennis A. Syomin and Barbara J. Finlayson-Pitts*

Department of Chemistry, University of California, Irvine, CA 92697-2025.
E-mail: bjfinlay@uci.edu; Fax: +1 949 824 3168; Tel: +1 949 824 7670

Received 15th August 2003, Accepted 29th September 2003
First published as an Advance Article on the web 21st October 2003

Nitrous acid (HONO) is the major source of OH in polluted urban atmospheres, so an understanding of its formation and loss processes both in urban atmospheres and in laboratory systems is important. Earlier studies over a limited range of conditions showed that HONO is taken up and undergoes reaction on surfaces. We report here a comprehensive set of studies of the decay of HONO and the formation of gas phase products over a range of initial HONO concentrations (0.1–11 ppm) at 1 atm pressure in N_2 at 296 K and 0, 20 and 50% relative humidity (RH), respectively. The loss of HONO and increase in gas phase products were measured over time using long path FTIR spectroscopy. Studies were carried out in an unconditioned borosilicate glass cell and in the same cell after pretreatment with dry gaseous nitric acid. In the HNO_3-conditioned cell, the loss of HONO was first order at all values of relative humidity (RH), and NO_2 was the only significant gas phase product. For the unconditioned cell, the reaction order increased from first order at 0% RH to second order at 50% RH. The gas phase products at 0% RH were equal amounts of NO and NO_2. The yield of NO increased to $>90\%$ at 50% RH while the yield of NO_2 decreased to $\leq 10\%$. For both the unconditioned and the HNO_3-treated cell, the rate of loss of HONO decreased with increasing RH. These results suggest that there is a competition between water, HONO and HNO_3 for surface sites. Displacement of HONO from the cell walls by water was observed in separate experiments. Possible mechanisms, and the implications for HONO formation in environmental chambers and in air, are discussed.

Introduction

Nitrous acid (HONO) is the major photochemical source of OH radicals in polluted urban atmospheres, both at sunrise and when averaged throughout the day.[1–5] Although the origin of the HONO has been somewhat controversial, it is believed that the heterogeneous NO_2 hydrolysis, described by overall reaction (1), is likely to be the major source:[6–11]

$$2NO_2 + H_2O \xrightarrow{\text{surface}} HONO + HNO_3 \qquad (1)$$

The nitrous acid is released to the gas phase; the nitric acid remains adsorbed on the surface.[12,13] However, the yield of HONO measured in laboratory studies is generally less than expected from reaction (1), particularly in reactors with large surface-to-volume (S/V) ratios.[10,14–24] This suggests either that some of the HONO reacts on the surface before it is released to the gas phase, or that it is released and subsequently reacts on the chamber walls.

Understanding the reactions of HONO on surfaces is important not only from a fundamental chemistry standpoint, but also for interpreting field and environmental chamber studies. Measurements of HONO and its precursor NO_2 in ambient air allow one to probe the contribution of heterogeneous reactions at the earth's surface to the production of HONO, and ultimately of OH, provided both the production and loss processes for HONO are understood.

In environmental chambers used to simulate reactions in air, the production of HONO has been observed from chamber walls,[11,25–29] even when oxides of nitrogen have not been included in the reaction mixture. Additionally, there have been several studies of the loss of HONO in laboratory systems.[18,30–35] Chan *et al.*[30,31] studied the decomposition in a stainless steel reactor ($S/V = 5.3\ m^{-1}$) at concentrations of HONO ranging from 2–9 ppm and at water vapor concentrations corresponding to 0.7–15% RH. They reported that the reaction is second order in HONO and occurs in the gas phase to generate NO and NO_2:

$$2\ HONO \leftrightarrow NO + NO_2 + H_2O \qquad (2)$$

In a number of subsequent studies, other groups also observed NO and NO_2 as products, but concluded that the reaction occurred heterogeneously on the reactor walls. For example, Kaiser and Wu[32] reported that the reaction occurred on the walls of a Pyrex reactor ($S/V = 63\ m^{-1}$) at RH from 0.2 to 5%, with a reaction order between one and two with respect to HONO. The rate of HONO loss decreased with increasing water vapor, with an apparent reaction order in water vapor of about −0.6. The production of NO and NO_2 were not consistent with reaction (2) alone and for analysis of the data, the reactions of HONO and NO with HNO_3 were included in their mechanism. These researchers found that prior exposure of the reactor walls to a mixture of NO, NO_2 and H_2O decreased the rate of HONO decomposition as the surface "aged", but that coating the reactor surface with boric acid increased the decomposition rate. In a separate study, Kaiser and Wu[33] studied the loss of HONO in the reactor in the presence of HNO_3, and concluded that the chamber walls play a role in the reaction between HONO and HNO_3. They observed the reaction to be first order in HONO as well as gas phase HNO_3, and the reaction rate decreased when the water vapor pressure was increased from 0.1 to 5 Torr, corresponding to a RH from 0.5 to 22% RH.

Jenkin *et al.*[18] studied the loss of HONO in a glass cell ($S/V = 13\ m^{-1}$) in conjunction with studies of the HONO

 DOI: 10.1039/b309851f

formation by reaction (1). They reported that the loss of HONO was first order at water vapor concentrations corresponding to 3.2 and 9.5% RH. Wallington and Japar[34] studied the decomposition of HONO in a similar reactor. They reported that the rate of disappearance of HONO increased in the presence of HNO_3 and could be modeled by a first order process in HONO. Ten Brink and Spoelstra[35] followed the loss of HONO in a Pyrex chamber at 80% RH. The decay of HONO was observed to be second order, with the major initial gas phase product being NO. At much longer reaction times ($\sim$ 60 hrs), NO_2 was also observed as a product. They reported that the results were the same at 50% RH.

In summary, the preponderance of evidence shows that the loss of HONO in laboratory systems occurs *via* reactions on the chamber walls. This is in agreement with theoretical studies[36] of reaction (2), which show that this reaction in the gas phase should be very slow, with a rate constant of $\sim 10^{-25}$ cm^3 molecule^{-1} s^{-1}. Furthermore, the rate and mechanism might depend on the nature and amounts of co-adsorbed species, including water.

With the exception of the Ten Brink and Spoelstra experiments,[35] previous studies have been carried out at relative humidities that are much lower than those found in the troposphere. In addition, there has been no comprehensive study of the heterogeneous decomposition of HONO in which the concentrations of HONO and co-adsorbed species such as water and nitric acid were systematically varied over a wide range. We report here the results of such experiments, using the walls of a borosilicate glass chamber as the surface, as in many of the previous studies. However, this material is also relevant to many surfaces found in the boundary layer, since windows, buildings, concrete *etc.* have high silicate contents.[10,37,38] We show that both water and HNO_3 compete with HONO for sites on the surface, which affects the kinetics, the products, and the mechanism of heterogeneous HONO uptake and reaction. This result has significant implications for HONO measurements in environmental chambers as well as in ambient air.

Experimental methods

Experiments were conducted at 296 K in a cylindrical, borosilicate glass, long-path cell equipped with a set of multi-pass optics of the White design.[39] Gas phase species were monitored using Fourier transform infrared spectrometry (Mattson, Research Series). The cell was 1.14 m in length, had an internal diameter of 0.15 m and a total volume $V = 19.4$ L. The optical pathlength in these experiments was 72 m. The flanges and inner supports consist of anodized aluminum that were coated with a thin coating of halocarbon wax (Halocarbon Products, Inc., Series 1500) to prevent contact of HNO_x with the metal surfaces. The surfaces of the gold-coated mirrors were coated with a protective layer of silicon monoxide. The surface area (S) of the cell, without the internal supports and optics, is 0.58 m^2 ($S/V = 30$ m^{-1}); when the surface area of the internal components is included, the total area is 0.89 m^2 ($S/V = 46$ m^{-1}). We have shown in recent studies[40] that halocarbon wax takes up water in amounts similar to borosilicate glass over a broad range of relative humidities. Thus, for reactions occurring on the cell surfaces, such as those described here, the total area including the optics is most relevant.

In a typical experiment, 4–50 Torr of a mixture of HONO in N_2 was introduced into the cell from the HONO generator described below. The pressure was then brought up to 1 atm with nitrogen at the desired RH value. Nitrogen was used as the diluent gas to minimize the potential for thermal oxidation of nitric oxide in the system by oxygen. The relative humidity was adjusted by varying the ratio of humid and dry nitrogen during filling of the chamber. The humid nitrogen was obtained by flowing N_2 gas through a bubbler containing Nanopure® water (Barnstead, 18.2 MΩ cm) and held at 296 K.

Concentrations of HONO, NO_2, and NO in the cell were measured as a function of time using FTIR spectroscopy. Spectra were collected at a resolution of 1 cm^{-1}, and 64 scans collected over 30 seconds were averaged for each data point. Gas phase HONO, NO_2 and NO were quantified by the net absorbance of their peaks at 1263, 2917 and 1875 cm^{-1}, respectively. Absolute concentrations of NO_2 and NO were based on calibrations using authentic samples in the cell. Nitrous acid concentrations were calculated from absorbances (base 10) using an effective cross section[41] of $(3.7 \pm 0.4) \times 10^{-19}$ cm^2 molecule^{-1} at 1263 cm^{-1}. Use of the effective cross section gives the total HONO concentration (*cis* and *trans* isomers, which are in equilibrium). (The 1263 cm^{-1} band that was measured is only due to the *trans* form.)

Two sets of studies were carried out using different treatments of the surfaces of the cell. In the first series, the cell walls were conditioned with gas phase HNO_3 by introducing approximately 2 Torr of dry gaseous HNO_3 into the cell. After $\sim$15 min, the cell was evacuated with a diffusion-pump for several hours. The HONO and humid N_2 were then added as described above. In the second series, the cell walls were unconditioned. At the beginning of this set of experiments the cell was thoroughly rinsed first with distilled and then with Nanopure® water to remove soluble contaminants. Subsequent experiments in this series were carried out after simply evacuating the cell for several hours with a diffusion pump, due to the impracticality of disassembling the cell, rinsing it and realigning the optics for individual experiments.

Nitrous acid was synthesized by reacting hydrochloric acid with sodium nitrite:

$$NaNO_2 + HCl \rightarrow HONO + NaCl \qquad (3)$$

Prior to reaction, the solid $NaNO_2$ (Aldrich, 99.5%) was exposed to humid N_2 (80–100% RH) for 15–20 min to moisten the salt surface. The flow of humid N_2 was then stopped and replaced by a flow of moist HCl in N_2, as obtained by flowing dry N_2 over the surface of an aqueous solution of HCl (Fisher, Certified ACS Plus, 12.1 M diluted $\sim$1:3 (v/v) with Nanopure® water).

Nitric acid used for conditioning the cell, and nitrogen dioxide and nitric oxide used for calibrations, were synthesized and purified as described elsewhere.[10]

Results

1. Experiments in an HNO_3-conditioned cell

Fig. 1 shows typical concentration–time profiles for HONO decay in an HNO_3 conditioned cell at 0 (Fig. 1a), 20 (Fig. 1c) and 50% RH (Fig. 1e), along with profiles for the gas phase products, NO and NO_2. Both NO_2 and NO are unavoidably present at the beginning of each experiment, due to HONO decomposition during its generation and handling in the glass manifold. This was particularly significant in experiments where the cell was conditioned with HNO_3 because the walls of the vacuum line used to introduce HONO into the cell had also been exposed to nitric acid. The data in Fig. 1 show that the only gas phase product observed in measurable yield is NO_2. The concentration of nitric oxide, present initially as an impurity, does not change significantly with time.

For each experiment, the initial rate of HONO loss and the corresponding rate of NO_2 formation were measured. The rate of HONO loss can be expressed by eqn. (I),

$$-\frac{d[HONO]}{dt} = k_d[HONO]^n \qquad (I)$$

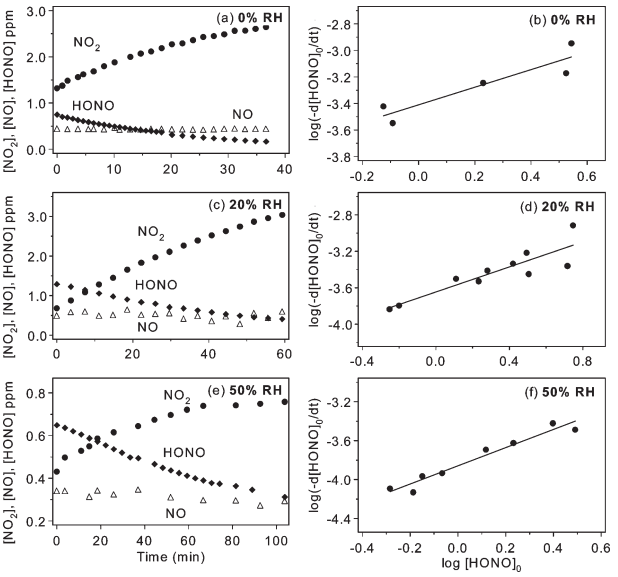

Fig. 1 Concentration–time profiles of HONO (◆), NO_2 (●) and NO (△) and corresponding plots of $\log(-d[HONO]_0/dt)$ *vs.* $\log[HONO]_0$ for HONO decay experiments at ~0% (a,b), 20% (c,d) and 50% RH (e,f) in the HNO_3 conditioned cell. Based on the known equilibrium constant for $2\ HONO \leftrightarrow NO + NO_2 + H_2O$,[30,31] equilibrium is not attained within the reaction times used here.

where n is the reaction order with respect to HONO and k_d the rate constant for HONO loss. This assumes that other species than HONO are not involved in the HONO loss (or that if they are, their concentrations are constant). The reaction order and rate constants for HONO decay were obtained from the slope and intercepts respectively of log-log plots of the initial rate of HONO loss *versus* the initial HONO concentration:

$$\log(-d[HONO]_0/dt) = \log k_d + n \log[HONO]_0 \qquad (II)$$

Figs. 1b, d and f show the log-log plots for 0, 20 and 50% RH, respectively. In all cases the reaction is approximately first order in HONO.

The data are summarized in Table 1. The first order rate constants (k_d) for loss of HONO decrease by a factor of approximately three in the range from 0 to 50% RH. The yield of NO_2 formed relative to HONO removed is between two and three at 0 and 20% RH, but falls to one at 50% RH.

2. Experiments in an unconditioned cell

Fig. 2a, c and e show typical concentration–time profiles for the decay of HONO and the formation of NO and NO_2 in the unconditioned cell at 0, 20 and 50% RH. At 0% RH, equal amounts of NO and NO_2 are produced. However, as the RH increases the relative yield of NO increases and that of NO_2 decreases.

Fig. 2b, d, and f shows the log–log plots (eqn. (II)) used to obtain the reaction order. The reaction is first order at 0% RH but changes to approximately second order at 50% RH. Table 1 also includes the data for these experiments. Because the reaction is first order only at 0% RH, the rate constant k_d is shown only for this set of experiments. However, it is clear from Fig. 2a, c and e that, as the RH increases, the rate of loss of HONO decreases.

Studies of the formation of HONO by the heterogeneous hydrolysis of NO_2, reaction (1), were previously carried out in this cell at values of RH up to 80%.[10] Based on these earlier experiments, HONO formation by heterogeneous NO_2 hydrolysis is negligible in comparison with the rate of HONO loss.

At low HONO concentrations (<0.9 ppm) and 50% RH in the unconditioned cell, HONO concentrations initially increased upon addition of the humid N_2, rather than decreased as was the case under all other conditions. This suggests that water competes with HONO for surface sites and displaces some HONO that was previously adsorbed onto the walls into the gas phase. To test this point, experiments were carried out in which the cell was first exposed for one hour at 50% RH to 13 ppm HONO and then pumped for 60 min. Dry N_2 was added up to 1 atm pressure and the gas composition monitored for 9.5 h. No production of gaseous HONO was observed during this time. The cell was then pumped out and N_2 at 50% RH added. Fig. 3 shows the concentration-time profile for HONO. Clearly, HONO is being produced in the gas phase, and the only available source is displacement by the competitive adsorption of water on the surface.

Discussion

For the reaction in the cell that had been pretreated with HNO_3, the reaction is approximately first order in HONO (Fig. 1), and NO_2 is the only gas phase product. Because the loss of HONO occurs on the surface of the cell, it is expected to be sensitive to the nature of the thin film of co-adsorbed

Table 1 Summary of HONO decomposition experiments

Conditioning of cell walls	RH (%)	No. of experiments	Range of initial $[HONO]_0$ (ppm)	Reaction order in $[HONO]_0$	First-order rate constant for HONO loss k_d (units of 10^{-4} s^{-1})	Yield of NO_2[c]	Yield of NO[d]
HNO_3							
	0	5	0.75–3.5	0.7 ± 0.3[a]	3.9 ± 1.1[a]	2.3 ± 1.0[b]	0
	20	10	0.56–5.6	0.7 ± 0.2	2.3 ± 0.6	2.8 ± 0.5	0
	50	8	0.52–3.1	0.9 ± 0.2	1.4 ± 0.2	1.1 ± 0.3	0
Unconditioned							
	0	12	0.11–10.9	1.1 ± 0.1	1.0 ± 0.2	0.59 ± 0.20	0.57 ± 0.13[b]
	20	10	0.31–4.1	1.5 ± 0.4	[e]	0.26 ± 0.26	0.67 ± 0.56
	50	7	1.3–10.9	1.8 ± 0.4	[e]	0.1 ± 0.1	1.1 ± 0.2

[a] Errors represent ± 2s. [b] Errors represent 95% confidence limits (CL) using the *t*-test. The 95 % CL is given by $ts/\sqrt{N}$ where the standard deviation $s = \sqrt{\sum(x_i - x_{av})^2/(N-1)}$ and N is the number of data points in the mean. [c] For the HNO_3-conditioned cell, the yield of NO_2 was calculated from the initial rates of NO_2 formation and HONO loss, i.e. from $\{d[NO_2]/dt\}/\{-d[HONO]/dt\}$. For the unconditioned cell where the rates of reaction were significantly slower, the yields were calculated from $\Delta[NO_2]/\Delta[HONO]$ at the end of each run; this was judged to be more accurate than using rates for the slower HONO losses. [d] The yields were calculated from $\Delta[NO]/\Delta[HONO]$ at the end of each run. [e] Since the reaction order is significantly greater than one, a first-order rate constant cannot be reported. However, as seen in Fig. 2, the rate of loss of HONO decreased with increasing RH.

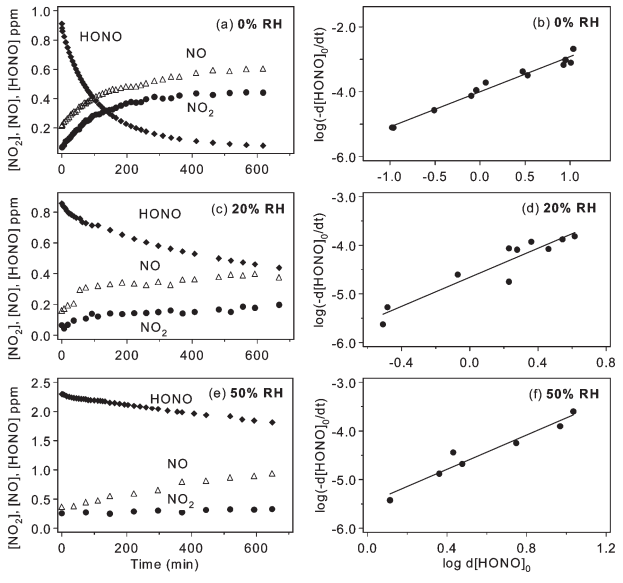

Fig. 2 Concentration–time profiles of HONO (◆), NO_2 (●) and NO (△) and corresponding plots of $\log(-d[HONO]_0/dt)$ *vs.* $\log[HONO]_0$ of HONO decay experiments at ~0% (a,b), 20% (c,d) and 50% (e,f) RH in the unconditioned cell. Based on the known equilibrium constant for $2\ HONO \leftrightarrow NO + NO_2 + H_2O$,[30,31] equilibrium is not attained within the reaction times used here.

species on the chamber walls. It is known from other studies in this laboratory that after exposing borosilicate glass to gas phase HNO_3, some of it remains adsorbed even after prolonged pumping.[10,38,42] The form of the acid on the surface is not known, but it is likely to be, at least in part, complexed to water.[10]

The production of NO_2 as the only gas phase product in the experiments where the walls were conditioned with HNO_3 is consistent with the uptake of HONO on the chamber walls, followed by its protonation by adsorbed nitric acid:

$$HONO_{(g)} \leftrightarrow HONO_{(ads)} \quad (4)$$

$$HONO_{(ads)} + HNO_{3(ads)} \rightarrow H_2O + NO^+ + NO_3^- \quad (5)$$

$$NO^+ + NO_3^- \rightarrow ONONO_2 \rightarrow 2\ NO_2 \quad (6)$$

If the HNO_3 adsorbed on the cell walls is constant, the rate of reaction of HONO should be first order in HONO, in agreement with observations.

Reactions (4)–(6) are the reverse of the heterogeneous hydrolysis of NO_2, reaction (1), which we recently proposed[10] to occur *via* formation of the asymmetric NO_2 dimer:

$$2\ NO_2 \leftrightarrow N_2O_4 \leftrightarrow ONONO_2 \quad (7)$$

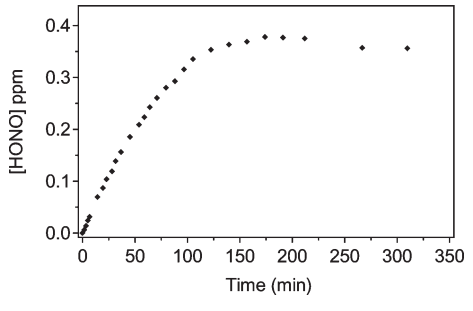

Fig. 3 Concentration–time profile of HONO in the HONO-conditioned cell at 50% RH and 1 atm in N_2. Before the experiment, the cell was exposed at 50% RH for 1 h to 13 ppm of HONO that contained 28 ppm of NO_2 and 60 ppm of NO as impurities. The cell was then pumped out before the water vapor-N_2 mixture was added.

The $ONONO_2$ then autoionizes and reacts with adsorbed water to generate HONO and HNO_3:

$$ONONO_2 \leftrightarrow (NO^+NO_3^-) \xrightarrow{H_2O} HONO + HNO_3 \quad (8)$$

This sequence can be driven in reverse by high initial concentrations of HONO and HNO_3 as used in the present study. The stoichiometry from reactions (4)–(6) is expected to be $\Delta[NO_2]/\Delta[HONO] = 2$. Our measured yields of NO_2 are 2.3 ± 1.0 and 2.8 ± 0.5 at 0 and 20% RH, respectively; the latter value is slightly larger than anticipated on the basis of the proposed mechanism. The yield of NO_2 at 50% RH falls to approximately one, and no additional gas phase products are observed. This suggests that, for every two HONO molecules that are taken up on the surface, one reacts to form NO_2 *via* the mechanism described above, while one remains on the surface as undissociated HONO, as the dissociated form of HONO ($H^+ + NO_2^-$), or as some as yet unidentified involatile product.

Nitrogen dioxide is known[43–46] to be generated in the decomposition of pure nitric acid, and indeed, some NO_2 formation was observed over time after the cell was pumped following the HNO_3 conditioning procedure. At 0% RH, the increase was small and represented less than 10% of the NO_2 formed in experiments where HONO was added. At 50% RH, significant amounts of NO_2 were generated, up to several ppm in 100 min. However, when HONO is present in the cell, its uptake and reaction with HNO_3 on the walls must compete with the generation of NO_2 from the self-reactions of adsorbed HNO_3. Thus, the NO_2 observed in the absence of HONO is an upper limit for the case where HONO is present. The fact that the yield of NO_2 falls to approximately one at 50% RH, compared to two at 0% RH, suggests that the contribution from the self-reactions of HNO_3 on the wall at the higher RH is not a major contributor to the measured NO_2 in the presence of added HONO.

A possible explanation for the low NO yields in the HNO_3-conditioned cell is that both NO and NO_2 are generated initially, but the NO reacts with adsorbed HNO_3,[33,47–56]

$$NO + 2\ HNO_3 \rightarrow 3\ NO_2 + H_2O \quad (9)$$

Based on earlier experiments in this laboratory in a different cell,[55,56] this process is expected to be too slow to be significant under the present experimental conditions. As a further check on this point, experiments were carried out at 0 and 50% RH in which 12 ppm of NO were added to the HNO_3 conditioned cell and the concentrations of gases monitored for 6 h. The observed rates of loss of NO and formation of NO_2 were confirmed to be too slow to be consistent with an initial formation of NO followed by reaction (9).

The data in Table 1 and in Figs. 1 and 2 show that the rate constant for HONO decomposition decreases with increasing relative humidity. As the partial pressure of water vapor increases, the amount of water on the surface increases relative to the amount of adsorbed nitric acid. The decreased rate constant at higher RH might be due to increased competition for the reaction of $NO^+NO_3^-$ with water to generate HONO and HNO_3. Alternatively, or perhaps in addition, increased adsorbed water could change the nature of nitric acid on the surface. Nitric acid exists in the undissociated, molecular form at low RH on silica surfaces.[12,13,57] Upon addition of water, dissociation to H^+ and NO_3^- occurs. This is consistent with gas-phase studies of complexes of nitric acid with water, where ionization of the acid occurs when there are four or more water molecules in the cluster with one nitric acid molecule.[58–60] A decrease in the rate constant with increasing RH would also result if molecular HNO_3 is the reactant, while the dissociated ionic form, whose concentration increases with more water on the surface, is unreactive.

In the unconditioned cell, the reaction was first order in HONO (Fig. 2b) at 0% RH with a rate constant that was about a factor of four slower than in the HNO_3-conditioned cell. In this case, nitric oxide and nitrogen dioxide were generated in equal yields, in contrast to the HNO_3 conditioned chamber where NO_2 was the sole gas phase product. As the RH increases to 50%, the rate of HONO loss decreases, the reaction order increases and the product changes to NO with a yield greater than 90%. This is in contrast to the reaction on the HNO_3-conditioned cell walls where the reaction order remained one and NO_2 was the only product over the 0–50% range of RH.

We propose that the experimental observations in the unconditioned cell are attributable to competition between HONO and H_2O for the available surface sites. Thus, as the water vapor concentration increases, the coverage of surface-adsorbed water increases. This leads to a decrease in the amount of adsorbed HONO, and hence in the rate of reaction. This conclusion is supported by the data in Fig. 3, where the addition of water to a cell previously exposed to HONO and then pumped out leads to an increase in HONO in the gas phase.

Further, a competition between water and HONO for surface sites is consistent with the change in reaction order from one to two as the water vapor concentration increases. Thus, in a system where both HONO and H_2O can be adsorbed on a surface, the fraction of the surface covered by HONO (θ_{HONO}) is given by eqn. (III),[61]

$$\theta_{HONO} = \frac{K^{HONO}[HONO]}{1 + K^{HONO}[HONO] + K^{H_2O}[H_2O]} \quad \text{(III)}$$

where K^{HONO} is the equilibrium constant for the surface uptake and desorption of HONO (*i.e.* $K^{HONO} = k_4/k_{-4}$ for reaction (4) above), K^{H_2O} is the corresponding equilibrium constant for adsorption of water and [HONO] and [H_2O] are the gas phase concentrations. In the absence of water vapor, eqn. (III) becomes

$$\theta_{HONO} = \frac{K^{HONO}[HONO]}{1 + K^{HONO}[HONO]} \quad \text{(IV)}$$

and if $K^{HONO}[HONO] \gg 1$, the fractional coverage of the surface by HONO becomes constant at one, *i.e.* the surface is saturated with HONO. In this case, the rate of reaction of gas phase HONO with adsorbed HONO is given by

$$-\frac{d[HONO]}{dt} = k'[HONO]_g[HONO]_{ads} = k'[HONO]S\theta_{HONO} = k'[HONO]S \quad \text{(V)}$$

where k' is the rate constant for the gas-surface reaction and S is the surface density of one HONO monolayer (molecule per cm^2). Because of the saturation of the surface by HONO, the reaction is predicted to be first-order in gas-phase HONO, which is consistent with our experimental observations.

At high relative humidities, water partially displaces HONO from the surface. Under conditions where $K^{H_2O}[H_2O] \gg K^{HONO}[HONO]$, eqn. (III) becomes

$$\theta_{HONO} = \frac{K^{HONO}[HONO]}{1 + K^{H_2O}[H_2O]} \quad \text{(VI)}$$

The rate of reaction of gas phase HONO with adsorbed HONO is then given by eqn. (VII):

$$-\frac{d[HONO]}{dt} = k'[HONO]S\theta_{HONO} = \frac{k'K^{HONO}[HONO]^2S}{1 + K^{H_2O}[H_2O]} \quad \text{(VII)}$$

That is, the loss of HONO from the gas phase decreases with increasing RH and becomes second order in HONO at constant RH, consistent with the experimental observations at 50% RH (Fig. 2e).

The fact that the rate appears to be between first and second order at intermediate relative humidities implies that the terms $K^{HONO}[HONO]$ and $K^{H_2O}[H_2O]$ are comparable under these conditions. Consider 20% RH, for example, where the water vapor concentration is about 5×10^3 ppm, and a 5 ppm HONO concentration. For the two terms $K^{HONO}[HONO]$ and $K^{H_2O}[H_2O]$ to be of comparable magnitude, K^{HONO} must be greater than K^{H_2O} by a factor of approximately 10^3.

The equilibrium constants for uptake of HONO and H_2O onto surfaces are related to the enthalpy and entropy of adsorption through the free energy. If it is assumed that the entropy of adsorption is similar for HONO and H_2O, then the ratio of the equilibrium constants is given by

$$K^{HONO}/K^{H_2O} = \exp[-(\Delta H_{ads}^{HONO} - \Delta H_{ads}^{H2O})/RT] \quad \text{(VIII)}$$

where ΔH_{ads}^{HONO} and ΔH_{ads}^{H2O} are the enthalpies of adsorption of HONO and water on the surface. If $K^{HONO}/K^{H_2O} \sim 10^3$, the difference between the enthalpies of adsorption of HONO and H_2O ($\Delta H_{ads}^{HONO} - \Delta H_{ads}^{H2O}$) must be approximately -17 kJ mol^{-1}.

Thompson and Margey[62] recently calculated enthalpies for formation of complexes of silica molecules (SiH_3OH or $Si(OH)_4$), taken as proxies for a silica surface, with HONO, water, HNO_3, NO_2 and N_2O_4. The enthalpy of formation for the complex of HONO with SiH_3OH was calculated to be -25.1 kJ mol^{-1}, and for the complex of H_2O with SiH_3OH, the enthalpy was calculated to be in the range from -15.5 to -23.2 kJ mol^{-1}, depending on the particular orientation of water to the silicate. This calculation shows that the difference in the enthalpies of adsorption for these complexes of HONO or H_2O should be in the range of - (2–10) kJ mol^{-1}. The difference for binding of HONO compared to H_2O to $Si(OH)_4$ was also small, ~ 2 kJ mol^{-1}. These differences are much smaller than our estimate of -17 kJ mol^{-1}. The apparent discrepancy could be due to several factors. First, the isolated SiH_3OH or $Si(OH)_4$ molecules used as proxies might not be truly representative of silica surfaces. This is particularly the case for borosilicate glass, which contains small amounts of oxides of metals such as Na, Zn, B, Al and Ti. Also, HONO may not adsorb in the molecular form by hydrogen bonding, as assumed in the calculations. For example, partial or full ionization to H^+ and NO_2^- would provide strong electrostatic interactions, with larger associated heats of adsorption.

This work also predicted[62] that nitric acid would form much stronger complexes with SiH_3OH and $Si(OH)_4$ than HONO. This might be the reason why HONO does not compete with HNO_3 for surface sites in the HNO_3-conditioned experiments, where the data are consistent with saturation of the surface sites by HNO_3.

The formation of equal amounts of NO and NO_2 as products is consistent with an autoionization reaction between gas-phase and adsorbed HONO:

$$HONO_{(g)} + HONO_{(ads)} \rightarrow NO^+ + NO_2^- + H_2O \quad (10)$$

$$NO^+ + NO_2^- \rightarrow N_2O_3 \rightarrow NO + NO_2 \quad (11)$$

Such autoionization reactions are known for HNO_3[43–45] as well as for N_2O_5[63–69] and N_2O_4 on ice.[70–72] In the case of HONO, the relatively large enthalpy of adsorption on the surface relative to water as discussed above suggests that the adsorbed species might already be partially or fully ionized.

As the RH increases in the unconditioned cell, the yield of NO increases and that of NO_2 decreases. At 50% RH, the yield of NO is greater than 90% (Table 1 and Fig. 2e). These observations are similar to those of Ten Brink and Spoelstra,[35] who studied the decay of HONO in a pyrex chamber at 80% RH and 1–10 ppm HONO. Typical data in Fig. 3 of that paper show NO as the major gas phase product in the first ~7 h of the reaction.

The mechanistic basis for the change in products as the RH increases in the unconditioned cell is not clear. In earlier studies[10] of the NO_2 heterogeneous hydrolysis we reported that the yield of HONO was less than 0.5 as expected from reaction (1), and that the "missing HONO" was replaced by gas phase NO. We proposed that this was due to the reaction of HONO with NO_2^+ on the surface,

$$HONO + NO_2^+ \rightarrow H^+ + 2\ NO + O_2 \qquad (12)$$

If this is the source of NO in the present experiments in the unconditioned cell at 50% RH, the NO_2^+ would have to be generated from adsorbed HONO if the reaction is to be second order as experimentally observed. However, a mechanism of formation of NO_2^+ on the surface from HONO is not clear.

In summary, most of the experiments reported here are consistent with our proposed mechanisms. The only observation for which a clear explanation is not available is the change in the product distribution in the unconditioned cell from equal amounts of NO and NO_2 at 0% RH to primarily NO at 50% RH. Further work is underway to clarify the mechanisms responsible.

To the best of our knowledge, this is the first comprehensive study of HONO reactions on a borosilicate glass surface in which both the initial HONO concentration and the RH were varied over a relatively wide range, including the impact of coadsorption of HNO_3. The data reported here agree in large part with previous studies carried out over a more limited set of conditions. For example, Chan *et al.*[30,31] reported that at low relative humidities in an unconditioned cell, NO and NO_2 are both generated and the rate of HONO loss decreases with RH, consistent with our experiments. We observed that the presence of HNO_3 increases the rate significantly and that the loss of HONO is first order under these conditions, in agreement with Kaiser and Wu[32] and Wallington and Japar.[34] Reaction orders between one and two have been reported, depending on the conditions and presence of HNO_3.[18,30–35] Our measured reaction orders are generally in agreement with these previous studies when comparisons are made under similar experimental conditions. For example, Jenkin *et al.*[18] measured the rate of HONO decay in a glass chamber of similar size to the one used in these studies and reported the loss was first order at RH corresponding to 3.2 and 9.5% and the absolute value of the first order rate constant was 3.7×10^{-4} s^{-1}. This is in excellent agreement with the value of $(3.9 \pm 1.1) \times 10^{-4}$ s^{-1} measured in the present studies where the loss was also first order.

Finally, the results presented here provide some insight into laboratory studies of the heterogeneous hydrolysis of NO_2 in which yields of HONO have been frequently measured to be less than expected based on reaction (1). The observation of increasing yields of NO with decreasing HONO yields at intermediate to high relative humidities in such studies of reaction (1)[10,14,15,17,23,24,73] is consistent with the formation of HONO followed by its conversion to NO on the "unconditioned" walls of the reactor as illustrated, for example, by the data in Fig. 2e.

Atmospheric implications

Nitrous acid production from the surfaces of environmental ("smog") chambers used for studying atmospheric reactions has been observed in many studies using different chambers.[25–29] This has been observed even when oxides of nitrogen have not been added during the experiment, implying that it must have arisen from contamination from previous experiments. Our studies show that the competition between water and HONO for surface sites leads to desorption of adsorbed HONO from the surface as the RH increases. This suggests that contamination of the walls of environmental chambers in previous experiments leaves adsorbed HONO (or comparable species such as H^+ and NO_2^-) on the surface, and that HONO is displaced by water when the RH value is increased. Hence, if this point is accepted, generation of HONO in such chambers will be unavoidable once the chamber walls have been exposed to oxides of nitrogen. Consistent with this explanation is the observation that the rate of generation of HONO in such chambers increases with RH.[29]

Nitrous acid has been measured in many field experiments, and it is clear from such studies that surface reactions act both as a source and as a sink for HONO. Separating the production and loss processes for HONO requires that the kinetics and mechanisms of this uptake be understood. In the tropospheric boundary layer there are a variety of surfaces of different chemical composition (*e.g.* vegetation, building materials *etc.*) available that might participate in uptake of HONO. Since many building materials are silicates,[37] our experiments using borosilicate glass are relevant to such surfaces in urban areas.

The results presented here suggest that the loss of HONO can vary from first to second order, depending on the RH and presence of reactive co-adsorbed species such as HNO_3. These experiments also show that HONO can be displaced from surfaces by water vapor, leading to an apparent increase in HONO as a function of RH. However, the formation of HONO from the NO_2 heterogeneous hydrolysis also increases with RH[10] so that measurements of HONO at different RH may be affected both by the dependence of reaction (1) on water and by the displacement of HONO from the surface through preferential adsorption of water.

Stutz and coworkers[74] have measured HONO and NO_2 in urban areas and find that their data are consistent with a first-order loss of HONO at RH from 10 to 100%. This suggests that urban surfaces may have sufficient deposited HNO_3 (or other species that are reactive towards HONO) that the kinetics for the loss of HONO are determined by the collision rate of HONO with the surface.

Acknowledgements

We are grateful to the California Air Resources Board (Contract No. 00-323) and the National Science Foundation (Grant No. ATM-0097573) for support of this work. We would also like to thank K. A. Ramazan, L. F. Phillips, L. M. Wingen, J. N. Pitts Jr. and J. Stutz for helpful discussions.

References

1 A. M. Winer and H. W. Biermann, *Res. Chem. Intermed.*, 1994, **20**, 423.
2 B. Alicke, U. Platt and J. Stutz, *J. Geophys. Res.*, 2002, **107**, 10.1029/2000JD000075.
3 J. Stutz, B. Alicke and A. Neftel, *J. Geophys. Res.*, 2002, **107**, 10.1029/2001JD000390.
4 X. Zhou, K. Civerolo, H. Dai, G. Huang, J. Schwab and K. Demerjian, *J. Geophys. Res.*, 2002, **107**, 10.1029/2001JD001539.
5 B. Aumont, F. Chervier and S. Laval, *Atmos. Environ.*, 2003, **37**, 487.
6 G. Lammel and J. N. Cape, *Chem. Soc. Rev.*, 1996, **25**, 361.
7 G. Lamme, *Formation of Nitrous Acid: Parameterization and Comparison with Observations*, Report No. 286, Max-Planck-Institut-für Meteorologie, Hamburg, 1999, pp. 1–36.
8 R. M. Harrison, J. D. Peak and G. M. Collins, *J. Geophys. Res.*, 1996, **101**, 14429.
9 V. R. Kotamarthi, J. S. Gaffney, N. A. Marley and P. V. Doskey, *Atmos. Environ.*, 2001, **35**, 4489.
10 B. J. Finlayson-Pitts, L. M. Wingen, A. L. Sumner, D. Syomin and K. A. Ramazan, *Phys. Chem. Chem. Phys.*, 2003, **5**, 223.

11 B. J. Finlayson-Pitts and J. N. Pitts, Jr., *Chemistry of the Upper and Lower Atmosphere: Theory, Experiments and Applications*, Academic Press, San Diego, 2000.
12 A. L. Goodman, G. M. Underwood and V. H. Grassian, *J. Phys. Chem. A.*, 1999, **103**, 7217.
13 W. S. Barney and B. J. Finlayson-Pitts, *J. Phys. Chem. A*, 2000, **104**, 171.
14 F. Sakamaki, S. Hatakeyama and H. Akimoto, *Int. J. Chem. Kinet.*, 1983, **15**, 1013.
15 J. N. Pitts, Jr., E. Sanhueza, R. Atkinson, W. P. L. Carter, A. M. Winer, G. W. Harris and C. N. Plum, *Int. J. Chem. Kinet.*, 1984, **16**, 919.
16 J. N. Pitts, Jr., T. J. Wallington, H. W. Biermann and A. M. Winer, *Atmos. Environ.*, 1985, **19**, 763.
17 R. Svensson, E. Ljungstrom and O. Lindqvist, *Atmos. Environ.*, 1987, **21**, 1529.
18 M. E. Jenkin, R. A. Cox and D. J. Williams, *Atmos. Environ.*, 1988, **22**, 487.
19 C. Perrino, F. DeSantis and A. Febo, *Atmos. Environ.*, 1988, **22**, 1925.
20 P. Wiesen, J. Kleffmann, R. Kurtenbach and K. H. Becker, *Faraday Discuss.*, 1995, **100**, 121.
21 J. Kleffmann, K. H. Becker and P. Wiesen, *Atmos. Environ.*, 1998, **32**, 2721.
22 J. Kleffmann, K. H. Becker and P. Wiesen, *J. Chem. Soc. Faraday Trans.*, 1998, **94**, 3289.
23 T. Wainman, C. J. Weschler, P. J. Lioy and J. Zhang, *Environ. Sci. Technol.*, 2001, **35**, 2200.
24 H. M. Ten Brink, J. A. Bontje, H. Spoelstra and J. F. van de Vate, in *Studies in Environmental Science*, ed. M. M. Benarie, Elsevier, Amsterdam, 1978, vol. 1, pp. 239.
25 W. P. L. Carter, R. Atkinson, A. M. Winer and J. N. Pitts Jr., *Int. J. Chem. Kinet.*, 1981, **13**, 735.
26 W. P. L. Carter, R. Atkinson, A. M. Winer and J. N. Pitts, Jr., *Int. J. Chem. Kinet.*, 1982, **14**, 1071.
27 F. Sakamaki and H. Akimoto, *Int. J. Chem. Kinet.*, 1988, **20**, 111.
28 W. A. Glasson and A. M. Dunker, *Environ. Sci. Technol.*, 1989, **23**, 970.
29 J. P. Killus and G. Z. Whitten, *Int. J. Chem. Kinet.*, 1990, **22**, 547.
30 W. H. Chan, R. J. Nordstrom, J. G. Calvert and J. H. Shaw, *Chem. Phys. Lett.*, 1976, **37**, 441.
31 W. H. Chan, R. J. Nordstrom, J. G. Calvert and J. H. Shaw, *Environ. Sci. Technol.*, 1976, **10**, 674.
32 E. W. Kaiser and C. H. Wu, *J. Phys. Chem.*, 1977, **81**, 1701.
33 E. W. Kaiser and C. H. Wu, *J. Phys. Chem.*, 1977, **81**, 187.
34 T. J. Wallington and S. M. Japar, *J. Atmos. Chem.*, 1989, **9**, 399.
35 H. M. Ten Brink and H. Spoelstra, *Atmos. Environ.*, 1998, **32**, 247.
36 A. A. Mebel, M. C. Lin and C. F. Melius, *J. Phys. Chem A*, 1998, **102**, 1803.
37 R. M. E. Diamant, *The Chemistry of Building Materials*, Business Books Limited, London, 1970.
38 A. M. Rivera-Figueroa, A. L. Sumner and B. J. Finlayson-Pitts, *Environ. Sci. Technol.*, 2003, **37**, 548.
39 J. U. White, *J. Opt. Soc. Am.*, 1942, **32**, 285.
40 A. L. Sumner, E. J. Mehnke, Y. Dubowski, J. T. Newberg, R. M. Penner, J. C. Hemminger, L. M. Wingen, T. Brauersand B. J. Finlayson-Pitts, 2003, submitted.
41 W. S. Barney, L. M. Wingen, M. J. Lakin, T. Brauers, J. Stutz and B. J. Finlayson-Pitts, *J. Phys. Chem. A*, 2000, **104**, 1692; W. S. Barney, L. M. Wingen, M. J. Lakin, T. Brauers, J. Stutz and B. J. Finlayson-Pitts, *J. Phys. Chem. A*, 2001, **105**, 4166.
42 A. L. Sumner, Y. Dubowski, R. C. Hoffman, D. J. Gaspar, E. Menke, J. T. Newberg, R. M. Penner, J. C. Hemminger and B. J. Finlayson-Pitts, unpublished data, 2003.
43 C. C. Addison, *Chem. Rev.*, 1980, **80**, 21.
44 J. Chédin, *J. Chim. Phys.*, 1952, **49**, 109.
45 E. Högfeldt, *Acta Chem. Scand.*, 1963, **17**, 785.
46 J. N. Crowley, J. P. Burrows, G. K. Moortgat, G. Poulet and G. LeBras, *Int. J. Chem. Kinet.*, 1993, **25**, 795.
47 J. H. Smith, *J. Am. Chem. Soc.*, 1947, **69**, 1741.
48 S. Jaffe and H. W. Ford, *J. Phys. Chem.*, 1967, **71**, 1832.
49 G. E. Streit, J. S. Wells, F. C. Fehsenfeld and C. J. Howard, *J. Chem. Phys.*, 1979, **70**, 3439.
50 I. R. McKinnon, J. G. Mathieson and I. R. Wilson, *J. Phys. Chem.*, 1979, **83**, 779.
51 A. C. Besemer and H. Nieboer, *Atmos. Environ.*, 1985, **19**, 507.
52 R. Svensson and E. Ljungström, *Int. J. Chem. Kinet.*, 1988, **20**, 857.
53 D. H. Fairbrother, D. J. D. Sullivan and H. S. Johnston, *J. Phys. Chem. A*, 1997, **101**, 7350.
54 M. Mochida and B. J. Finlayson-Pitts, *J. Phys. Chem. A*, 2000, **104**, 9705.
55 N. Saliba, H. Yang and B. J. Finlayson-Pitts, *J. Phys. Chem. A*, 2001, **105**, 10 339.
56 N. Saliba, M. Mochida and B. J. Finlayson-Pitts, *Geophys. Res. Lett.*, 2000, **27**, 3229.
57 A. L. Goodman, E. T. Bernard and V. Grassian, *J. Phys. Chem. A*, 2001, **105**, 6443.
58 B. D. Kay, V. Hermann and A. W. J. Castleman, *Chem. Phys. Lett.*, 1981, **80**, 469.
59 X. Zhang, E. Mereand and A. W. J. Castleman, *J. Phys. Chem.*, 1994, **98**, 3554.
60 J. J. Gilligan and A. W. J. Castleman, *J. Phys. Chem. A*, 2001, **105**, 5601.
61 R. I. Masel, *Principles of Adsorption and Reaction on Solid Surfaces*, John Wiley & Sons, New York, 1996.
62 K. C. Thompson and P. Margey, *Phys. Chem. Chem. Phys.*, 2003, **5**, 2970.
63 M. Mozurkewich and J. Calvert, *J. Geophys. Res.*, 1988, **93**, 15 889.
64 A. Fried, B. E. Henry and J. G. Calvert, *J. Geophys. Res.*, 1994, **99**, 3517.
65 C. George, J. L. Ponche, P. Mirabel, W. Behnke, V. Scheer and C. Zetzsch, *J. Phys. Chem.*, 1994, **98**, 8780.
66 W. Behnke, C. George, V. Scheer and C. Zetzsch, *J. Geophys. Res.*, 1997, **102**, 3795.
67 G. N. Robinson, D. R. Worsnop, J. T. Jayne, C. E. Kolb and P. Davidovits, *J. Geophys. Res.*, 1997, **102**, 3583.
68 A. Wahner, T. F. Mentel, M. Sohn and J. Stier, *J. Geophys. Res.*, 1998, **103**, 31 103.
69 F. Schweitzer, P. Mirabel and C. George, *J. Phys. Chem. A*, 1998, **102**, 3942.
70 J. Wang, M. R. Voss, H. Busse and B. E. Koel, *J. Phys. Chem. B*, 1998, **102**, 4693.
71 J. Wang and B. E. Koel, *J. Phys. Chem. A*, 1998, **102**, 8573.
72 J. Wang and B. E. Koel, *Surf. Sci.*, 1999, **436**, 15.
73 C. England and W. H. Corcoran, *Ind. Eng. Chem. Fundamen.*, 1974, **13**, 373.
74 J. Stutz, personal communication, 2003.